

DEVELOPMENT AND EXPERIENCES WITH A FULLY-DIGITAL HANDHELD MAPPING SYSTEM OPERATED FROM A HELICOPTER

J. Vallet^{a,*}, J. Skaloud^b

^a EPFL, Laboratory of Photogrammetry, CH-1015 Lausanne, Switzerland – julien.vallet@a3.epfl.ch

^b EPFL, Laboratory of Topometry, CH-1015 Lausanne, Switzerland – jan.skaloud@epfl.ch

Commission I, WG I/5

KEY WORDS: Photogrammetry, Disaster, Mapping, CCD, GPS/INS, LiDAR, Integration, Acquisition.

ABSTRACT:

This paper presents a self-contained, light and flexible mapping system that can be quickly deployed into inaccessible areas. Although designed to measure wind-transported snow volumes and the avalanche mass balance over an experimental site, the system is suitable to any large-scale 3-D terrain mapping. The system is comprised of supporting electronics that is loosely linked to a light but ridged sensor block containing digital camera, Lidar, an IMU and a GPS antenna. The relatively small size and weight of the sensor block permits manual pointing of the camera and the Lidar either towards the mountain face or the valley bottom. Such hand-held steering allows mapping of the avalanche/land slides release and deposit zones during the same flight with an optimal geometry. At the same time it dampens the engine-induced vibrations on the sensors. The installation time of the system in a helicopter is less than 15 minutes and its re-installation does not require new calibration. The exterior orientation (EO) parameters of the camera and laser are determined directly by GPS/IMU integration. Optionally, the orientation performance of the navigation solution may be improved by integrating the data from the second GPS antenna placed on the helicopter tail. Once the system is calibrated (once per sensor assemblage) and with EO determined for both sensors, an automated DTM and orthophoto generation can be achieved. The practical experience with CCD/GPS/INS has demonstrated a mapping accuracy of 10cm and 15cm in the horizontally and vertically, respectively. The performance of recently added Lidar is under evaluations.

1. INTRODUCTION

1.1 Motivations

Switzerland is making an effort to improve its preventative measures against natural disasters. In the cycle of integrated risk management, the steps of intervention and reconstruction following a disaster are studied, and then the phase of rebuilding is followed by implantation of prevention methods. Each of these phases attempts to reduce certain risks and impact of a natural catastrophe.

In this context, observation methods for certain phenomena and their impact on the land and infrastructure are essential in order to optimize certain processes and to make correct decisions. Surveying instruments, photogrammetry and, more recently, laser and radar systems have been integrated into surveillance platforms in an effort to examine zones which are at particularly high risk. Including these observation methods in the process of integrated risk management demands systems of particularly high performance. For example, it is essential that the transfer of data (motion, coordinates, image, digital terrain model) occur quickly and without delay in order to ensure the smooth continuation of the entire data collection process.

The objective of this research is to produce a cartographic system that can be rapidly deployed in the event of a catastrophe. This concept of near real-time cartography is very important for those attempting to intervene during such events.

1.2 System Requirements

The designed system aims to fulfil the following requirements:

- Fast set-up and availability (minutes or hours)
- Relative independence from a particular carrier
- Possibility to map near vertical (mountain faces) and horizontal (valley bottoms) features during the same flight with uniform accuracy
- High relative and absolute mapping accuracy (<20cm)
- No assistance of ground control points
- Fast delivery time for DTM and orthophoto generation (few hours after flight)

1.3 Evolution of a System Concept

The modern mapping and remote sensing tools can be classified according to three basic criteria:

- Precision, resolution and sensitivity
- Deployment speed, mapping speed and product delivery turn-around time
- Instrumentation cost and carrier dependence

The trade-off between these conditions gave a rise to different systems as depicted in Figure 1. The development of the EPFL system called HELIMAP started in 1999 as a response to the need of SLF-Davos (Swiss Federal Institute for Snow and Avalanche Research) in mapping avalanches and snow transport (Issler, 1999). The emphasis was placed on high resolution and accuracy (10-15cm), low cost and system portability (i.e. independence from a carrier, Skaloud and Vallet, 2002).

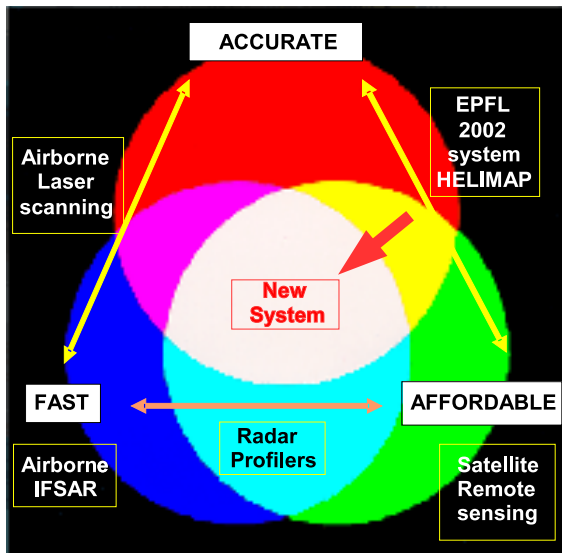


Figure 1: The spectrum of modern mapping tools. The system combines the best characteristics across different technologies.

The sensor choice was a high-quality portable photogrammetric camera that is now replaced by high-resolution digital camera, with a quality similar to most commercial systems (Mostafa and Hutton, 2003). The enabling technology for achieving mapping autonomy is the integration of high-accuracy GPS receivers with inertial navigation system (INS) that allows tracking the 3D motion of the image sensor in space and time.

In other words, thanks to GPS/INS, a pair of photographs is all that is needed to map scenery. The sensor block is light and small enough to be hand-held by an operator. Therefore, the installation on the helicopter is very quick and a flying mission can be quickly executed over any type of terrain. Although precise and quick in acquisition, the process of creating elevation models from photographs is relatively slow. The approach is therefore less suitable in applications where time matters, such as risk evaluation.

Apart from other important benefits listed in Table 1, integrating an airborne laser scanner (ALS) into the actual system can effectively eliminate this setback. A combination of GPS/INS and Lidar data has the potential to provide an almost automated generation of the Digital Surface Model close to real-time. Other advantages, such as the spectral (intensity) observations, are independent of illuminations and are also of great value.

CCD/GPS/INS	CCD/ALS/GPS/INS
Autonomous	Automation of 3D map generation
Uniform accuracy	24 hours operation
Fine details, texture, ortho-photo	Intensity image (spectral characteristics)
Fast deployment	Quick mapping (day or hours)
Carrier (helicopter)	Uses custom integration and of-the-shelf sensors \Rightarrow reasonable cost

Table 1: Benefits of laser scanner inclusion

No matter what the benefits are, the high acquisition cost of complete Lidar systems (>1000K USD) cannot be balanced by sporadic system use on small surfaces. Moreover, the portability of the traditional laser scanning system between different carriers is limited because of specific demands (e.g., floor view) and the long set-up time. Hence, the cost of maintaining a designated system carrier is therefore another prohibiting factor for such type of application. An alternative solution by mandating a third-party service provider is not suitable due to the need of system availability on a short-time notice. Finally, the accuracy in mountains, where generally disasters occur, is poor for fixed systems due to unfavourable geometry (Favey, 2001; Vallet, 2002).

To maintain the benefits of Lidar while keeping the total cost of sensor around 100K USD, a combination of a previously developed system (Vallet, 2002) with a medium range (~500m) Lidar has been undertaken. Moreover, the market release of mid format digital cameras in 2002 offered the possibility to create a fully digital mapping system of decimetre accuracy at reasonable cost.

The choice of a helicopter as the system carrier is justified by its capability to fly close to the ground at low speed. This allows capturing photographs in large-scale and provides better flight line navigation. In the following, particularities of the system will be described together with an analysis of its performance.



Figure 2: The handheld block composed of all the devices: digital camera, laser scanner, GPS antenna and IMU.

2. SYSTEM DESCRIPTION

Similarly to its former version (Skaloud and Vallet, 2002; Vallet, 2002), the current system combines several sensors into a single block: a digital camera, an inertial measurement unit (IMU), a GPS antenna and recently, an airborne laser scanner (Lidar). The sensors are rigidly mounted on a light and compact carbon-aluminium frame. The block of sensors is handheld and thus offers large manoeuvrability while maintaining constant relative

orientation between them (Figure 2). Moreover, the system remains modular and, depending on the needs, units can be easily removed. Following are the main three operational modes:

1. Camera + GPS: 4.5 kg
2. Camera + GPS/IMU: 6kg
3. Camera + GPS/IMU + Lidar: 12 kg

2.1 Imagery

The digital camera is composed of the Hasselblad Biogon SWCE 903 camera with a focal length of 38mm that is attached to a digital back (Kodak ProBack Plus). The size of the CCD chip is 4072x4072 pixels with 9µm pixel size. A home made electronic device controls the synchronization of the CCD with the shutter aperture by generating a pulse that is time-registered in the GPS receiver. The choice of the lens was based on its low distortion, a comparison of MTF curves and field tests. Images are stored on two internal 4GB Flashcards that allow taking up to 800 shots.

2.2 Airborne Laser Scanner (ALS)

The Lidar scanner unit is either the LMS-Q140i-60 or the newer model LMS-Q240-60. Both models are manufactured by Riegler and differ mainly in the maximum measurement range and interfaces. The laser wavelength of 900µm fits well measurements of natural targets and above all the snow covered surfaces. The maximum range is around 500m and the range resolution is 25mm. The scanner performs up to 80 scan lines per second at 10 kHz data rate. The rotating mirror induces a swath of 60° that corresponds well to the field of view of the digital camera that is 55°. Data are synchronized thanks to PPS pulse of the GPS receiver and a standard PC governs their storage through Ethernet or ECP ports.

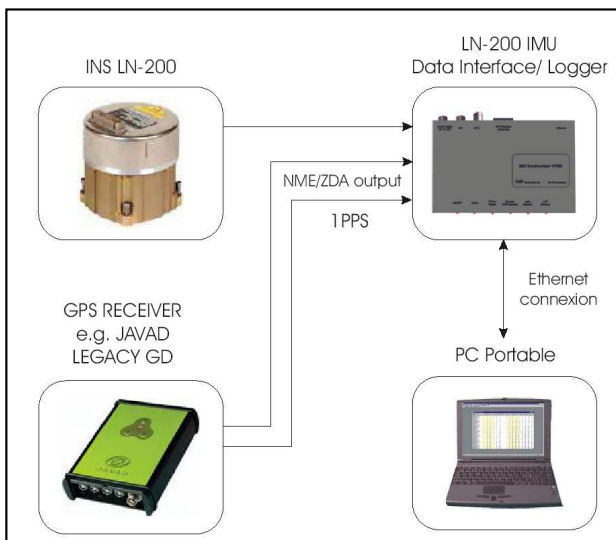


Figure 3: Data flow and synchronization for the IMU/GPS units.

2.3 Navigation devices for sensor's georeferencing

As with the use of sensors, the system remains modular in accommodation of navigation devices, namely the GPS receivers and the IMU. The system currently employs a Javad Legacy GD GPS receiver on board of the helicopter and additional GPS receivers on the ground. Positive experience has also been made with the Leica's SR530 receivers. In its most basic setup (CCD + GPS) the GPS data collection rate is set to 5 Hz, which is

sufficient sampling rate for the dynamic of a helicopter. This rate is reduced to 1 Hz or less when IMU is employed.

The IMU is tactical-grade strapdown inertial system (LN-200 A1) with 400Hz measurement rate. The IMU data are synchronized through small custom interface (Viret, 2003) and sent via Ethernet link to a standard portable PC as schematically depicted in Figure 2. Again, modularity was in the design priorities here, and thus the GPS receivers as well as the PC are easily interchangeable in case of hardware failure. The recorded IMU data are used in a post-mission integration with the differential carrier phase GPS data via a Kalman Filter employing 25 to 30 states.



Figure 4: The system in action with Alouette III helicopter. The holder for supporting the system weight during transition flights is located under operator's right leg.

2.4 Helicopter mount

The helicopter mount (Figure 4) is independent from its carrier, which has several advantages. First, the installation time is as short as a few minutes. Second, changing carriers does not require re-calibration of the sensors. Third, its flexible handling allows maintaining optimal geometry of the sensors in steep and flat terrains for the benefit of higher mapping accuracy. Finally, most of the rotor-induced vibrations are dampened when the operator holds the system and activates the imaging sensors (Skaloud and Vallet, 2001). An additional simple holder can be added to the exterior of the helicopter to support the system during approach flights.

2.5 Flight management

The system is designed to map smaller areas at large-scale, which permits a simple but efficient flight management concept. The system operator conducts photograph overlap and shots timing whereas the navigator/pilot steers along the flight line. The flight-line navigation uses the display of a rugged PC running PenMap™ software accepting the NMEA/GGA message sent by the GPS receiver. Receivers like Javad GD benefit of WAAS/EGNOS capability, which guarantees sufficient navigation accuracy in speed and position for manual aiming of the camera and laser sensors.

3. SYSTEM CALIBRATION

The system calibration can be divided into a few basic steps:

- Lever arm calibration: finding the linear offsets between each measurement unit
- Boresight calibration: determining the angular offsets between the IMU and the sensors due to mounting
- Interior calibration: finding or re-fining parameters related to sensors' interior orientation (Lidar, camera).

In principle, all these steps can but do not have to be calibrated in-flight (Colomina, 1999; Kruck, 2001). In-flight calibration is convenient, but may not deliver the desired accuracy when the correlation between the estimated parameters remains significant. In the following, we demonstrate how the calibration accuracy (and thus mapping) improves when at least the lever arm calibration is performed separately and time correlation of the IMU derived attitude is properly considered.

3.1 Lever arms

Thanks to the small separation between instruments, the lever arms relating the camera projection centre to GPS antenna phase centre, the IMU navigation centre and the laser measurement origin can be determined in laboratory with mm-level accuracy. This is accomplished using tacheometric measurements and terrestrial photogrammetry. Instead of mounting the GPS antenna, IMU and the laser on the frame, three steel needles materialize the physical centres of these sensors. A calibration polygon of about twenty targets is captured with the camera mounted in the frame from three different positions. For each position, the needles are surveyed with a theodolite in the coordinate system with known relation to the calibration polygon. A self-calibration bundle adjustment is performed on the image set (Kruck, 2001) to obtain the coordinates of the projection centre and the orientation of the camera with respect to the lab-frame. Parameters of interior orientation may be also estimated this way, although with lower accuracy. With this method, the lever arms are determined in the camera-frame with accuracy better than 1cm.

In the following we compare the above 'exact' method with other convenient, albeit less precise approaches:

- In-flight estimation of the camera-GPS lever arm by the rigorous approach of integrated bundle adjustment (Kruck, 2001) with and without control points.
- In-flight estimation of the camera-GPS lever arm by comparing the AT-derived projection centre with GPS antenna coordinates (needs control points).
- In-flight estimate of GPS-IMU lever arm as additional states in GPS/INS Kalman Filter.

Method	Error in lever arm [cm]			
	X	Y	Z	σ
A: with control points	0.4	0.2	3.5	2
A: with no control pts.	1.3	5.0	26	36
B: AT/GPS – 2 steps	0.2	3	4	17
C: GPS/INS – KF	5.0	18	30	2

Table 2: Error in lever arm estimates when compared with laboratory values in camera (A+B) and body frames (C).

Table 2 summarizes the results. Just the estimates of the first (A) approach agree well with the laboratory values but only when a

significant number of control points is used. The estimated lever arm between GPS-IMU observation centres by approach (C) is also inaccurate although the flight included several figure-eight turns to decorrelate the relations among the Kalman Filter states. Determining the lever arm with respect to laser scanner in-flight is even more problematic. Hence, since neither of the considered in-flight methods offers satisfactory solution, the lever arm values should be determined in lab rather than estimated from airborne data.

3.2 Boresight

Unlike the lever arms, the boresight angles are difficult to estimate in laboratory with adequate accuracy, although methods to do so have been proposed (Bäumker and Heimes, 2001). This is mainly due to the difficulty of achieving good IMU-alignment without inducing sufficient dynamic. Here, in-flight calibration offers the best solution.

For the best simultaneous estimate of boresight angles for camera and Lidar we propose flying over a rectangular building with a flat roof in two perpendicular stripes in both directions at different scales. The area may or may not be equipped with accurate Ground Control Points (GCPs), however the latter improves the estimate. As for the camera, three approaches have been considered before selecting the most accurate one (Skaloud and Schaer, 2003):

- One-step procedure: the INS/GPS attitude and position are introduced as additional observations into the bundle adjustment and the boresight angles are estimated together with the parameters of exterior and interior orientation (Kruck, 2001).
- Traditional two-steps procedure: AT including the GPS or GPS/INS coordinates of the camera projection centre is performed in self calibration mode and the camera orientation is compared with INS/GPS attitude at each photograph. The differences are formed, and boresight angles are computed as their (weighted-) average.
- Modified two-step procedure: As method II while accounting for the time correlations in the IMU data. As these correlations are significant (Figure 5), the changed weighting scheme provides unbiased boresight estimate with realistic level of confidence.

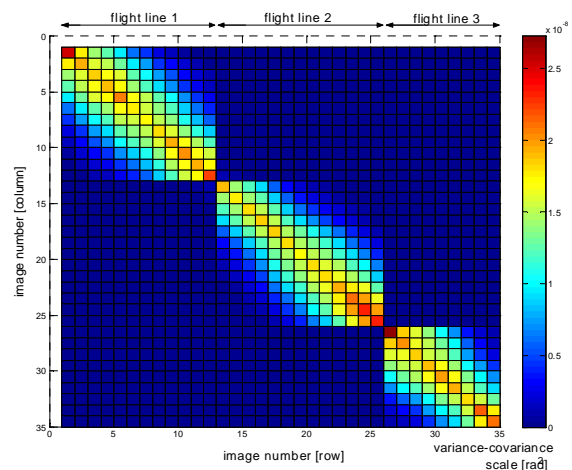


Figure 5: Q_{II} weighting matrix with IMU temporal correlations.

A small numerical comparison of three approaches is given below. The test zone consisted of approximately 3x7 image block and 24 check-points ($\sigma=3\text{cm}$). The tie points were measured manually and the AT-GPS aided solution was used as an input to the '2-step' procedure (with and without time correlation). In parallel '1-step' boresight determination was calculated. As can be seen from Table 3, the 1-step (I.) and 2-step (II.) estimates have similar mean values when no temporal correlations are considered. Both approaches are also too confident in the resulting accuracy. On the other hand, considering the temporal correlation in IMU rises the estimate uncertainty that becomes more realistic for the given type of IMU. However, at the same time, the mean is closer to the correct value, which in turn increases the mapping accuracy as shown in the next section and in Table 5.

Method	Calibration Flight 1:10000 Boresight Estimation					
	Estimated MEAN [deg]			Estimated ACCURACY [deg10 ⁻³]		
	roll	Pitch	yaw	r	p	y
I: 1-step	-0.003	-0.311	0.242	3	3	3
II: 2-step without time correlation	-0.003	-0.310	0.240	2	1	2
III: 2-step using correct correlation	-0.004	-0.309	0.235	6	3	10

Table 3: Boresight results according to the employed method

As for the Lidar's boresight, the final procedure has yet not been finalized but main steps can be briefly outlined:

- Stereoplotting of breaklines on the building roof tops
- Extracting the corresponding lines from the laser points
- Adjusting the plotted and laser-detected lines in each direction of flight yields the sought boresight angles.

4. SYSTEM PERFORMANCE

The HELIMAP system has undergone several years of experience in the first two modes of operation (Section 2). Its quality is appreciated in frequent flying missions related to natural hazards applications. The functionality and merits of adding ALS became apparent during a feasibility test that was realized in February 2004. As the evaluation of this data set has yet not been completed, we turn our focus to CCD based sensor.

4.1 Imagery

The change from analogue to digital camera (Vallet, 2002) was supported by field and laboratory experiments. Comparisons between the digital images and the digitized photos revealed that digital sensors provide sharper and less noisy images than a film-based imagery as shown in Table 4.



	Digital	Digitized Film
Transition B/W	½ pixel 1.5gsv	3-4 pixels 6gsv
Noise (1 σ)		

Table 4: Comparison of digital/analogue photos in terms of sharpness and noise (gsv = grey scale value).

The higher image quality of a digital camera allows reducing the scale two times with respect to analogue camera without losing the details. This fact partially compensates for the smaller format of the CCD sensor, which requires taking significantly more photos to cover the same area.

4.2 Mapping Accuracy

The following evaluation will focus on the system absolute accuracy at discrete points. A test field divided in two areas of about 25 and 12 GCPs, respectively, will serve the purpose. The scale of the images that were taken over this test field varies from 1:9000 to 1:11000 and the accuracy of ground control points is at 2cm level. As some GCPs are not specially signalized, the measurement of their image coordinates may introduce additional error from 4 μm to 8 μm (i.e. 3-8cm in the object space).

Method	Constraints		RMS at GCPs [cm] application field		
	GCP	Block	σ_0 [μ]	X,Y	Z
AT	•	•	2	4	4
AT-GPS		•	2	9	10
GPS / INS	I: 1 step		10	12	15
	II: 2 step no corr.		9	15	17
	III: 2 step + time corr.		7	10	14

Table 5: Comparison of mapping accuracy between different approaches to EO determination with an indication of operational constraints.

The indirect (AT, AT/GPS) and direct (GPS/INS) approaches to photogrammetric mapping are compared in Table 5 in terms of empirically estimated accuracy. The direct georeferencing by GPS/INS is further evaluated with respect to the different methods of boresight estimation as presented in the previous section. It is apparent that accounting for temporal correlation in IMU data during boresight estimate (Table 3) reduces image residuals and improves accuracy of object coordinates. Although the RMS values for the direct method are slightly higher than those for the indirect approach, the demand for providing 20cm-level mapping accuracy or better is fulfilled. The benefits of direct georeferencing are, however, numerous, as it avoids many difficulties that arise when performing automated AT in mountainous terrain. Adopting this method also considerably increases the operational flexibility needed in natural disaster mapping. The AT-GPS approach remains an interesting option for areas where GCP's are difficult to implement, but the relief and texture allows successful automation of tie point measurements procedure. Obviously, the merits of using ALS for fully automated DTM generation are apparent, but the method is still under evaluation.

4.3 Cost considerations

The cost of the mapping system is an important and sometimes a decisive factor for its adoption. Apart from counting the value of hardware (Table 6), the cost evaluation should also consider the amount of work related to each mode of system operations (Table 7). As can be seen from Table 7, the image orientation and DTM generation can rarely be automated in 'non-standard' scenarios involving steep terrain. As these tasks are time consuming, their liberation by Lidar well justifies the supplementary hardware cost of USD 35K. The total equipment costs amount to approximately USD 100'000. This is almost an order of magnitude lower than

that of most of the turnkey commercial systems. In other words, the cost of a development leading to a modular fully digital large scale mapping system of decimetre accuracy has been justified.

Equipment	Cost [US\$]
Digital Camera	30'000
GPS receivers	13'000
IMU (LN-200 A1)	20'000
Lidar (LMS-Q140i-60)	35'000
IMU interface	3'000
Frame	2'000
Computer	2'000
TOTAL HARDWARE COST:	105'000

Table 6: System equipment cost.

OPERATION MODES	GEOREFERENCING			PRODUCTS	
	GCP	Tie points	Navigation	DTM	Ortho-photo
AT	• M	• M	-	• M	• A
AT-GPS	-	• M	• A	• M	• A
Direct (CCD/GPS/IMU)	-	-	• A	• M	• A
CCD/GPS/IMU/ALS	-	-	• A	• A	• A

Table 7: Comparison of processing tasks (M: manual, A: automated) for different modes of system operation.

5. CONCLUSIONS AND OUTLOOK

The development of a dedicated airborne mapping system (HELIMAP) was initiated as a response to the country's needs for natural risk management and monitoring. The objective was to design a self-consistent system, easily deployable on a helicopter that can provide digital surface mapping of an area of interest:

- With a high precision (0.2m),
- With a high resolution (<1m²),
- Shortly after the flying mission (few hours).

This information is essential for risk assessment and monitoring of natural hazards such as avalanches, debris and water flows, floods, as well as forestry management. Evolution of the system followed the emergent technologies used in modern mapping and remote sensing. First, the analogue camera has been replaced with a CCD sensor to increase the image quality. Second, airborne laser scanner was added to drop the need for photogrammetric stereoploting.

At the same time new approaches were investigated in the direct georeferencing, especially with respect to boresight and lever arm calibration. It was concluded that surveying lever arms in laboratory is superior to in-flight calibration, which should be reserved for determining boresight and parameters of interior-orientation. Moreover, the significance of considering temporal correlation in the IMU/GPS data with respect to the boresight determination was highlighted in a newly developed procedure.

The mapping experience with the system in CCD/GPS/IMU mode has proven its unique performance in terms of flexibility, cost and

accuracy (<20cm). To improve the production time and hopefully fully automate the mapping process, a Lidar has been integrated to the system. However, the evaluation of the new ALS/CCD/GPS/IMU operation mode has not yet been finalized.

ACKNOWLEDGEMENTS

We would like to thank Ulrich, Weismann + Rolle AG for their active contribution to the system conception and flight expertise. Many thanks to Air Glaciers helicopter company for their availability and flexibility during the frame design and test flights.

REFERENCES

Bäumker, M. and F.J. Heimes, 2001. New Calibration and Computing Method for Direct Georeferencing of Image and Scanner Data Using the Position and Angular Data of an Hybrid Inertial Navigation System. in Integrated Sensor Orientation, Proc. of the OEEPE Workshop. Hanover: CD-ROM.

Colomina, I., 1999, GPS, INS And Aerial Triangulation: What Is The Best Way for The Operational Determination of Photogrammetric Image Orientation, in Proc. ISPRS Comm. III, München. p. 212-130.

Favey, E., 2001. Investigation and improvement of airborne laser scanning technique for monitoring surface elevation changes of glaciers. *Dissertation ETH n° 14045*. Zurich.

Kruck, E., 2001, Combined IMU and sensor calibration with BINGO-F. in Integrated Sensor Orientation, Proc. of the OEEPE Workshop". Hannover: CD-ROM.

Issler, D., 1999. European avalanche test sites. Overview and analysis in view of coordinated experiments. *Mitteilungen #59*, 1999. SLF Davos.

Mostafa M., Hutton J., 2003. Emerge DSS: A Fully Integrated Digital System for Airborne Mapping Mostafa – calibration. *ISPRS International Workshop on Theory, Technology and Realities of Inertial / GPS Sensor Orientation, Commission 1, WGI/5, Castelldefels, Spain, 22.-23. September.*

Skaloud, J., Vallet, J., 2002. High accuracy handheld mapping system for fast helicopter deployment. *International symposium on Geospatial Theory, ISPRS Comm IV*. Ottawa, Canada, 9-12th July 2002.

Skaloud, J., Schaer, P., 2003. Towards a more rigorous boresight calibration. *ISPRS International Workshop on Theory, Technology and Realities of Inertial / GPS Sensor Orientation, Commission 1, WGI/5, Castelldefels, Spain, 22.-23. September.*

Vallet, J., 2002. Saisie de la couverture neigeuse de sites avalancheux par des systèmes aéroportés. *Ph.D. Thèse n°2610*, EPF Lausanne, Switzerland.

Viret, P., 2003. Development of a Miniaturized Inertial Data Logger, *Master Thesis*, TOPO, EPF Lausanne, Switzerland. <http://www.vnrsa.ch/products/LN200.htm>